Soil & Tillage Research 194 (2019) 104322

Contents lists available at ScienceDirect

Soil & Tillage Research

journal homepage: www.elsevier.com/locate/still

An integrated approach to exploring soil fertility from the perspective of rice (*Oryza sativa* L.) yields

Huifeng Wang[a,b], Lipeng Yao[c], Biao Huang[a,*], Wenyou Hu[a], Mingkai Qu[a], Yongcun Zhao[a]

[a] Key Laboratory of Soil Environment and Pollution Remediation, Institute of Soil Science, Chinese Academy of Sciences, Nanjing 210008, China
[b] University of Chinese Academy of Sciences, Beijing 100049, China
[c] Nanjing Municipal Research Institute of Environmental Protection, Nanjing 210019, China

ARTICLE INFO

Keywords:
Multimodels
Fuzzy mathematical theory
Spatial statistics

ABSTRACT

Soil fertility should be explored from a productivity perspective because the most important function of the soil is to ensure crop yield. This study presents an integrated and scientific approach to exploring soil fertility based on rice (*Oryza sativa* L.) yields, using Jinxian County as an example. The main soil types are Haplic Acrisols and Hydragric Anthrosols. Five soil fertility indicators (p-Value < 0.05) were selected according to the generalized additive model (GAM) hypothesis test between the rice yield and each indicator. Furthermore, these indicators were used to assess the quality of soil fertility via Takagli and Sugeno (T-S) fuzzy neural networks models. Finally, the geodetector model was used to explore the restricting indicators of soil quality that can influence rice yields. The results indicate that continuous fertilization for decades has improved the surface soil organic matter (SOM) concentrations in the study area. However, the surface total potassium (K_T) was still low at a mean value of 13.95 ± 4.74 mg/kg. The determination power (DP) of exchangeable magnesium (0–20 cm) and K_T (20–40 cm) of 0.067 and 0.061, respectively, revealed that the proper use of potassium and magnesium fertilizers can increase rice yields. This integrated soil fertility exploration could scientifically assess the soil fertility and identify mainly restricting indicators of soil fertility in the study area. Moreover, these effective models with minor adjustments could be applied to assess soil fertility in other typical areas.

1. Introduction

Soil fertility represents the capacity of soil productivity, ensures crop yield, and establishes a foundation for sustainable agriculture (Merrill et al., 2013; Yao et al., 2015; Kaniu and Angeyo, 2015). Crop growth and production status is one of the most important characteristics for assessing soil fertility (Juhos et al., 2016; Vasu et al., 2016). A restricting indicator analysis of soil quality could provide the theoretical basis and technical support for sustainable agricultural production and management. Therefore, to integrally and thoroughly explore soil fertility from a productivity perspective, a soil fertility assessment and the restricting indicator analysis should be undertaken (Zhang et al., 2016; Rojas et al., 2016).

The first step in a soil fertility assessment is the selection of soil fertility indicators. A number of traditional approaches for selecting indicators have been proposed, such as the Delphi method (Nelson et al., 2009), multiple linear regression, and principal component analysis (Qi et al., 2009). Multiple linear regression and principal component analysis are commonly used. Multicollinearity may exist among the interpreted variables of a multiple linear regression, and it often severely affects parameter estimation, which increases the model error and invalidates the robustness of the model (Toebe and Filho, 2013). Although the principal component regression method can eliminate multicollinearity via a complicated calculation process to reshape the variables, it is more reliable and accurate for identifying the most informative independent variable (Rahmanipour et al., 2014). The reshaped variable is not the same as the dependent variables; thus, the relationship of the dependent and independent variables may be irrelevant, which leads to unreasonable results. The generalized additive model (GAM) which was proposed by Hastie and Tibshirani (1986), can circumvent the problems above. The advantage of GAM is that raw data can determine the essence of independent variables and dependent variables rather than requiring early assumptions. More dependent variables result in more accurate results. Because it is especially useful for analyzing and complex problems, such as various ecological problems (Amosa and Majozi, 2016; Yi et al., 2016), this model could also efficiently and accurately describe the corresponding relationship between rice (*Oryza sativa* L.) yield and soil fertility indicators. Then,

* Corresponding author.
E-mail address: bhuang@issas.ac.cn (B. Huang).

https://doi.org/10.1016/j.still.2019.104322
Received 26 April 2018; Received in revised form 30 December 2018; Accepted 29 June 2019

significant correlation indicators could be extracted to represent the soil fertility indicators.

Based on the selected soil fertility indicators, a soil fertility quality assessment can be achieved (Raiesi, 2017; Liu et al., 2016). However, soil quality is an uncertain or fuzzy environmental issue in a complex natural ecosystem. Fuzzy mathematical theories can provide more rigorous and realistic estimations for imprecise and complex nonlinear systems (Rodríguez et al., 2016), which can lead to more reliable and objective assessments (Blanes et al., 2017). Common assessment models have been combined with fuzzy inference systems, such as fuzzy mathematics (Yan and Luo, 2016), fuzzy logic systems (Rodríguez et al., 2016), and Takagli and Sugeno (T-S) fuzzy neural networks (Zhang, 2012), etc. The advantage of the T-S fuzzy neural networks model is its ability to simulate complex nonlinear systems with fewer rules and the continuous modification of the membership function of fuzzy subsets (Xu et al., 2013).

An important component of soil fertility is exploring restricting indicators based on determination power (DP) analysis. DP analysis can be performed by traditional statistical methods, such as dimensionality reduction, correlation, and fitting, which can provide suggestions for soil regionalization and agricultural production. Along with the development of remote sensing (RS), geographic information system (GIS), and global position system (GPS) technology, spatial statistics analysis from assumption of spatial dependency have played an important role in environmental research (Wang and Xu, 2017). The geodetector model presented by Wang et al. (2010) has obvious advantages when evaluating the DP of geographic issues affected by the spatial distribution of environmental indicators (Hu et al., 2014). Therefore, geodetector models are superior for analyzing the DP of soil fertility indicators that affect crop yield from a productivity perspective.

The Poyang Lake Plain is a well-known rice cultivation area in China. Since the 1980s, many studies have examined the quality of soils and conducted restricting indicator analyses in the Poyang Lake region, and they have demonstrated that certain indicators, such as acidification and the potassium deficiency, could influence rice production in this area (Lai et al., 1989; Jiang et al., 2010; Yao et al., 2015). Thus, a scientific assessment of soil quality and an exploration of restricting indicators based on rice yields could provide a theoretical basis for further improving land productivity. Jinxian County, located on the Poyang Lake Plain in southeast China, was selected as the study area. The primary purpose of this study was to perform an integrated soil fertility exploration in Jinxian County. The detailed purpose were: (1) to use GAM hypothesis test to select soil fertility indicators in combination with rice yields in Jinxian County; (2) to provide an integrated fuzzy assessment of quality of soil fertility based on the above indicators; and (3) to analyze the restricting indicators of soil fertility that affect the rice yield.

2. Materials and methods

2.1. Description of the study area and sampling

Jinxian County is affiliated to Nanchang City, Jiangxi Province, southeast China. It is located in the southern area of Poyang Lake between latitudes 28°09′41″ and 28°46′13″N and longitudes 116°01′15″ and 116°33′38″E, with a total area of 1971 km^2 (Fig. 1). The study area is a typical hilly lakeside area. Low hills and plains are located in the central and western area, and alluvial plains occur near the water in the northern area. The mean annual sunshine is 1936 h, the mean annual temperature is 17.5 °C, and the mean precipitation is 1587 mm. The main soil types are Haplic Acrisols and Hydragric Anthrosols (WRB, 2015). Fluvic Cambisols and Haplic Phaeozems are also present in this area (WRB, 2015). Agricultural soil accounts for approximately 43,067 ha and the main crop is rice.

The distributions of soil sampling sites (Fig. 1) were planned based on the soil types, spatial distribution uniformity, and yield distribution. To avoid the influence of fertilization on rice cultivation and yield prediction, soil samples were collected after the rice harvest and before the beginning of the next tillage, in October 2012. The total number of soil samples was 103. In addition, the cutting ring samples were collected to determine the soil bulk density. The geographic coordinates of the sampling sites were recorded using a handheld GPS (GARMIN GPSMAP® 64 st).

We combined rice yields in the study area to perform an integrated soil fertility assessment that was representative and and biologically relevant. According to the phenological patterns of rice growth, Landsat-7 Enhanced Thematic Mapper Plus (ETM+) and Landsat-8 Operational Land Imager (OLI) imagery were used to interpret the rice planting area. All satellite imageries used in this study were obtained from the United Stated Geological Survey (http://earthexplorer.usgs.gov/). Then, the normalized difference vegetation index (NDVI) in the study area was acquired. Finally, using the established fitting model of the measured rice yields and the corresponding normalized NDVI, rice yields of the entire study area was measured.

2.2. Chemical analysis

Soil bulk density (BD) was calculated by the ratio between soil dry mass and core volume (Viana et al., 2014). The soil particle composition included clay (particle size < 0.002 mm), silt (particle size range between 0.05-0.002 mm), and sand (particle size range between 2-0.05 mm), and it was measured via the pipette method (Lu, 2000). Soil pH was measured using potentiometry ((Huang et al., 2006). The concentration of soil organic matter (SOM) was measured using the Walkley-Black method (Nelson et al., 1996). The cation exchange capacity (CEC) was measured using the ammonium acetate method, and the exchangeable calcium (Ex.Ca), sodium (Ex.Na) and magnesium (Ex.Mg) were determined based on extraction with ammonium acetate and ethylene diamine tetraacetic acid (EDTA) and measured according to the inductively coupled plasma (ICP) method (Fan et al., 2017). The total nitrogen (N_T) concentration was measured using the Kjeldahl method (Liu et al., 2017); briefly, the soil samples were digested using an acid mixture of HF, $HClO_4$, and HCl for analysis of total phosphorus (P_T) and total potassium (K_T). Then, the digested sample solutions were analyzed using the Mo-Sb colorimetric method and flame photometry method, respectively (Zhang et al., 2016). The available phosphorous (P_{AV}) concentration was measured using $NaHCO_3$ extraction and the Mo-Sb colorimetric method (Wolde and Haile, 2015); the available potassium (K_{AV}) concentration was measured with ammonium acetate extraction and the ICP method (Zhang et al., 2016). The available nutrition trace elements of copper (Cu), iron (Fe), manganese (Mn), and zinc (Zn) were measured by diethylenetriaminepentaacetic acid (DTPA) extraction and inductively coupled plasma atomic emission spectrometry (ICP-AES) (Fan et al., 2017).

2.3. Analysis method and algorithm

2.3.1. Generalized additive model to select soil fertility indicators

GAM is an extended model based on the generalized linear model, it uses a link function to handle the nonlinear relationship between response variables and a smoothing function of multiple explanatory variables, and it does not require presupposed parameters (Yi et al., 2016). This model is more flexible and suitable for variable data types and for statistical distributions of characteristics. The equation of the model is as follows (Wu et al., 2015):

$$g(\mu) = b_0 + \sum_{j=1}^{p} f_j(x_j) \tag{1}$$

where $\mu = E[Y|X]$, $g(\mu)$ is the link function, b_0 is the constant intercept item, and $f_j(x_j)$ is the smoothing function for describing the relationship between $g(\mu)$ and the explanatory variables of number j.

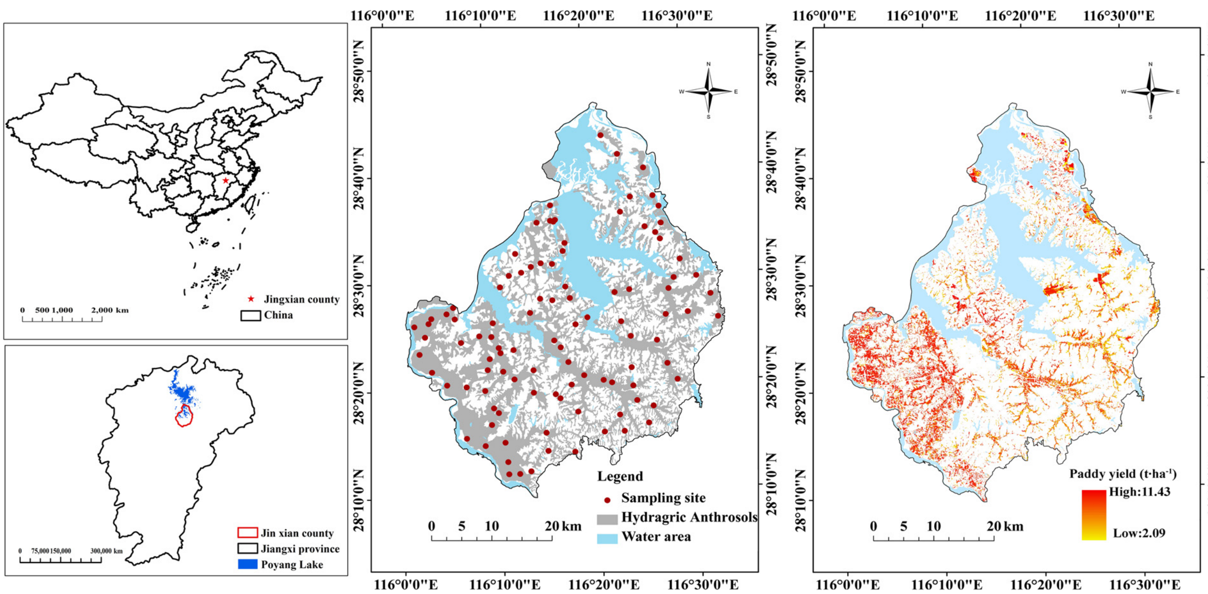

Fig. 1. Geographic positions of the soil sampling sites and the rice yield in the study area.

Table 1
Generalized additive model (GAM) hypothesis test results between the rice yield concentration and single indicators.

Explanatory variables	*F*	*p*-Value	R^2
Total potassium (0-20 cm)	9.4	0.003 **	0.08
Exchangeable magnesium (0-20 cm)	6.5	0.012 *	0.05
Exchangeable sodium (0-20 cm)	8.4	0.005 **	0.07
Total potassium (20-40 cm)	9.3	0.003 **	0.07
Exchangeable sodium (20-40 cm)	6.1	0.015 *	0.05
DTPA-Mn (20-40 cm)	2.4	0.018 *	0.14

DTPA-Mn : Available manganese (Mn) was measured by diethylenetriaminepentaacetic acid (DTPA);
0–20 cm : Soil layer 0–20 cm (surface soil);
20–40 cm : Soil layer 20–40 cm (subsurface soil).

We used the function ‘gam’ of package ‘mgcv’ in R 3.2.3 developed by Wood (2006) to model the response of rice yields to the various soil physical and chemical parameters. Six indicators were identified as explanatory variables that had a significant influence on rice yields (*p*-value below 0.05) in Table 1. K_T (0–20 cm), Ex.Na (0–20 cm), and K_T (20–40 cm) had significant influences (*p*-value below 0.01). In contrast, the *p*-values of the other indicators were above 0.5, indicating no significant influence. The degree of freedom values of all of the selected variables were 1, meaning that all of the soil fertility indicators had a linear relationship with rice yields.

Generalized additive model (GAM) hypothesis test results between the rice yield concentration and single indicators.

2.3.2. Determination of the assessment criteria

The key to modeling realistic conditions was to determine subjection functions and turning points with biological relevance. The standard core functions and cutoff values were measured through the relationship between remote sensing images and the rice yield. The distribution was established according to a scatterplot and the trend line of the average rice yield with the soil fertility indicators (Fig. 2). Then, the lower (L) and upper (U) limit values were confirmed by the standard deviation of curves multiplied by -1 and 1, respectively. The trend of DTPA-Mn (20–40 cm) with the rice yield was inconsistent with the actual trend, and it was likely to be affected by multiple other indicators. Therefore, we removed DTPA-Mn (20–40 cm) from the indicators in the soil fertility assessment. Within a certain range, the higher indicators corresponded to higher yields, and when the indicator exceeded a certain threshold, the crop yield did not increase. The classification criteria based on the above screening process and divisions are listed in Table 2. According to the criteria, we assessed the soil fertility quality of Jinxian County and separated the soil into three grades. Grade I represented the best level, and grade III represented the worst level.

2.3.3. Assessment based on the T-S fuzzy neural network model

The T-S fuzzy neural network model not only updates automatically but also corrects the membership functions of fuzzy subsets. This model provides rapid convergence and explicit physical meaning because it combines the characteristics of the fuzzy logic system and neural network.

The T-S fuzzy logic system uses the "IF–THEN" form to define rules. When the rule was R^i, the fuzzy inference was as follows (Hou, 2011; Song et al., 2018):

$$R^i\text{: if } x_1 \text{ is } A_1^i,\ x_2 \text{ is } A_2^i, \ldots, x_k \text{ is } A_k^i \text{ then } y_i = p_0^i + p_0^i x_1 + \ldots + p_k^i x_k$$

where A_k^i is the fuzzy set of fuzzy systems, $p_k^i (k = 1, 2, \ldots, j)$ represents the fuzzy system parameters, y_i is the output based on the fuzzy rules. In addition, the input is the fuzzy part, and the output is the certain part. This fuzzy inference indicates that the output is the first combination of inputs. The inference includes four layers: the input layer, blurring layer, inference layer, and output layer.

Layer 1: Assumed input $x = [x_1, x_2, \ldots, x_k]$ (2)

Layer 2: We calculate the membership degree of x_k based on the fuzzy rule:

$$m_{A_k^i} = \exp\left(-\frac{(x_k - c_k^i)}{b_k^i}\right) \quad k = 1, 2, \ldots, j;\ i = 1, 2, \ldots, n \tag{3}$$

where c_k^i and b_k^i are the center and width of the membership functions, respectively; k represents the input parameters; and n is the number of fuzzy subsets.

Layer 3: The membership degree is fuzzy calculated by continued multiplication with the fuzzy operator:

$$w^i = m_{A_k^1}(x_1) * m_{A_k^2}(x_2) * \ldots m_{A_k^i}(x_k) \quad i = 1, 2, \ldots, n \tag{4}$$

Layer 4: The above fuzzy model is used, to calculate the output y_i:

$$y_i = \sum_{i=1}^{n} \omega^i (p_0^i + p_0^i x_1 + \ldots + p_k^i x_k) / \sum_{i=1}^{n} \omega^i \tag{5}$$

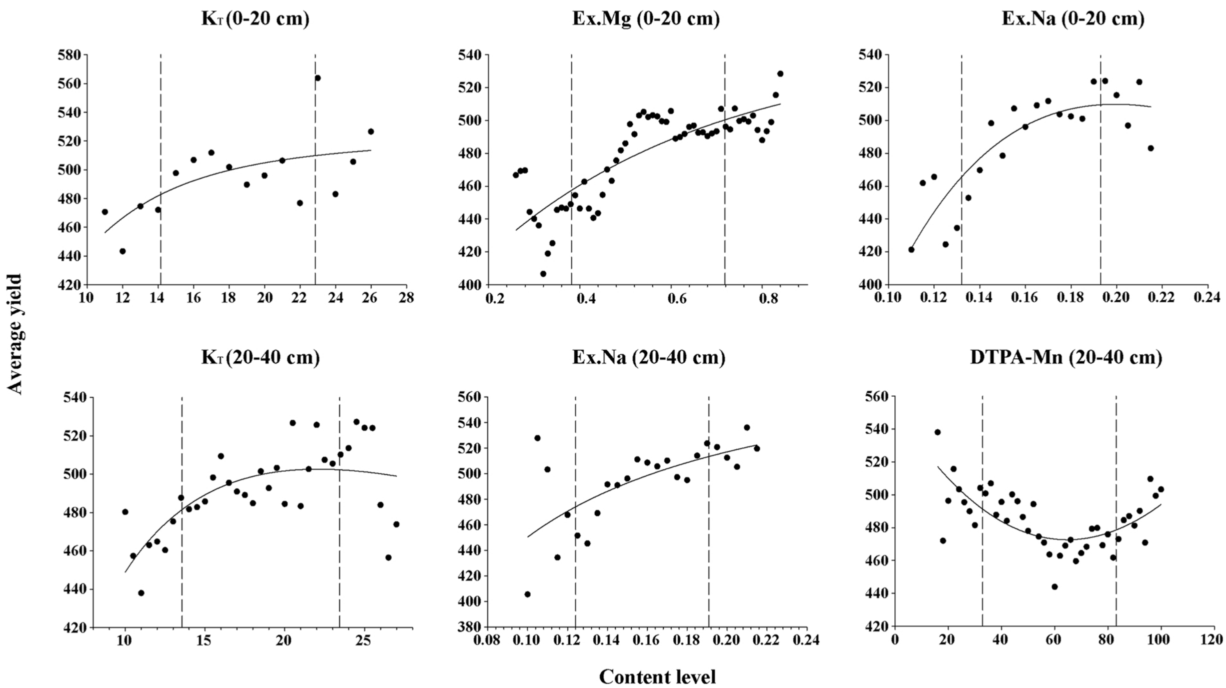

Fig. 2. Statistics of the measured rice yield with different levels and cutoff values of fitting functions of soil fertility indicators in Jinxian County.

Table 2
Assessment standard of soil fertility quality.

Indicator	Grade I	Grade II	Grade III
Total potassium (0-20 cm)	(22.8, +∞)	(14.2,22.8)	(014.2)
Exchangeable magnesium (0-20 cm)	(0.71, +∞)	(0.38,0.71)	(0,0.38)
Exchangeable sodium (0-20 cm)	(0.192, +∞)	(0.132,0.192)	(0,0.132)
Total potassium (20-40 cm)	(23.4, +∞)	(13.6,23.4)	(013.6)
Exchangeable sodium (20-40 cm)	(0.190, +∞)	(0.124,0.190)	(0,0.124)

0–20 cm : Soil layer 0–20 cm (surface soil);
20–40 cm : Soil layer 20–40 cm (subsurface soil);

The learning algorithm of the T-S neural network is as follows:
1) Error calculation:

$$e = \frac{1}{2}(y_d - y_c)^2 \tag{6}$$

where y_d is the expected output of the model, y_c is the actual output of the model, and e is the error of the expected output against the actual output.
2) Coefficient modification:

$$p_k^i(j) = p_k^i(j-1) - \alpha\frac{\partial_e}{\partial_{p_k^i}} \tag{7}$$

$$\frac{\partial_e}{\partial_{p_k^i}} = (y_d - y_c)\omega^i / \sum\nolimits_{i=1}^{n} \omega^i \cdot x_k \tag{8}$$

where p_k^i is the coefficient of the neural network, α is the learning rate of the network, x_k is the input parameter, and ω^i is the continued multiplication of the input parameters.
3) Parameter modification:

$$c_k^i(j) = c_k^i(j-1) - \beta\frac{\partial_e}{\partial_{c_k^i}} \tag{9}$$

$$b_k^i(j) = b_k^i(j-1) - \beta\frac{\partial_e}{\partial_{b_k^i}} \tag{10}$$

where c_k^i and b_k^i are the center and width of the membership functions, respectively.

2.3.4. Geodetector model

The distribution of most geographic variables and their indicators on the spatial scale obeyed a certain rule. A similar spatial distribution pattern between a geographic variable and an indicator indicates a direct or indirect relationship between the indicator and the geographic variable. Then, the DP of the indicator on the spatial distribution of the geographic variable can be calculated. According to the mechanism, the geodetector model was first applied to detect the characteristics affecting endemic disease (Wang, et al., 2010).

In the present study, this model was used to the detect DP for the rice yield based on the soil fertility indicators. Both the rice yield and the soil fertility indicators were polygon data that had different spatial units. To match the two variables in space, our uniformly dispersed the rice yield in the spatial zone was overlaid with the distribution of indicators, and then each discrete point of the dependent variable and independent variable values was extracted (Wang and Xu, 2017).

In the study area, a 1 km × 1 km grid was set in ArcGIS 10.0. Then, we extracted the measured value of the rice yield in the grid (Figure S1a). After the points without value were eliminated, each point was set to Y in Figure S1b. Soil fertility indicators, as X variables of the model, should be interpolated and extracted by the Y. The X variables were the five soil fertility indicators selected by GAM. These indicators were divided into three groups according to their classification information. In the present study, we set the total potassium (K_T) as an example of X variable to interpolate and divide it into grades I, II, and III based on Table 2 and then extract by the rice yield points (Y) (Figure S1c).

To analyze the spatial relationship between Y and X, we first overlaid the layers in Figures S1b and 1c. The variances of K_T in grades I, II, and III were represented by $Var_{K_{T1}}$, $Var_{K_{T2}}$ and $Var_{K_{T3}}$, respectively.

The DP value of K_T to the rice yield can be expressed as follows:

$$P_{D,U} = 1 - \frac{1}{n\sigma_U^2}\sum\nolimits_{i=1}^{m} n_{D,i}\sigma_{U_{D,i}}^2 \tag{11}$$

where $P_{D,U}$ is the DP of K_T to the rice yield; $n_{D,i}$ is the number of K_T samples in grades I, II, or III; n is the number of samples in the whole study area; m is the number of grade areas (m = 3 in this example); σ_U^2 is the variance of the rice yield in the whole zone; and $\sigma_{U_{D,i}}^2$ is $Var_{K_{T1}}$, $Var_{K_{T2}}$ and $Var_{K_{T3}}$. By assuming that $\sigma_{U_{D,i}}^2 \neq 0$, the model was established. $P_{D,U} = 1$ means that the rice yield is completely affected by

Table 3
Statistics of soil characteristics in Jinxian County.

Item	Range[a]	Mean ± SD[b]	CV[c](%)	Range	Mean ± SD	CV (%)
	Surface soil (0–20 cm)			Subsurface soil (20–40 cm)		
pH	4.32 - 6.14	4.80 ± 0.29	6.04	4.41 - 7.14	5.52 ± 0.54	9.86
SOM (g/kg)	11.37 - 47.03	33.63 ± 6.71	19.96	4.06 - 44.97	15.49 ± 7.67	49.47
N_T (mg/kg)	1.14 - 2.96	1.96 ± 0.42	21.62	0.32 - 2.46	0.98 ± 0.40	40.91
P_T (mg/kg)	0.44 - 1.19	0.66 ± 0.16	23.77	0.22 - 1.08	0.44 ± 0.14	31.67
K_T (mg/kg)	7.62 - 31.71	13.95 ± 4.74	33.96	7.26 - 30.69	14.10 ± 4.78	33.94
P_{AV} (mg/kg)	10.35 - 134.27	36.77 ± 20.65	56.16	2.10 - 40.09	11.45 ± 8.36	73.03
K_{AV} (mg/kg)	22.50 - 235.50	60.71 ± 33.80	55.69	17.75 - 168.32	52.08 ± 32.96	63.29
CEC (cmol/kg)	6.31 - 16.32	10.23 ± 2.12	20.77	3.73 - 13.97	8.90 ± 2.11	23.75
Ex.Ca (cmol/kg)	1.29 - 7.11	3.01 ± 1.19	39.50	1.00 - 64.59	4.46 ± 6.14	137.66
Ex.Mg (cmol/kg)	0.16 - 1.41	0.55 ± 0.21	38.38	0.18 - 8.91	0.83 ± 0.85	101.93
Ex.Na (cmol/kg)	0.08 - 0.30	0.15 ± 0.04	28.82	0.07 - 0.27	0.14 ± 0.04	28.74
DTPA-Fe (mg/kg)	88.33 - 447.93	255.72 ± 77.03	30.12	6.51 - 411.93	89.08 ± 81.40	91.38
DTPA-Mn (mg/kg)	4.09 - 201.91	39.76 ± 39.06	98.23	6.03 - 239.91	57.19 ± 45.45	79.48
DTPA-Cu (mg/kg)	1.22 - 8.54	3.69 ± 1.11	30.17	0.24 - 8.46	2.07 ± 1.35	65.19
DTPA-Zn (mg/kg)	0.65 - 5.75	2.23 ± 0.98	43.75	0.19 - 3.93	0.83 ± 0.74	89.13
BD (g/cm^3)	0.76 - 1.39	1.08 ± 0.13	12.08	1.03 - 1.76	1.51 ± 0.15	9.77
Silt/Clay (%)	0.33 - 4.27	2.51 ± 0.62	24.58	0.90 - 5.18	2.39 ± 0.63	26.36

Range : Minimum value - maximum value;
SD : Standard deviation;
CV : Coefficient of variation;
SOM : Soil organic matter;
N_T, P_T and K_T : Total concentrations of nitrogen, phosphorus and potassium;
P_{AV} and K_{AV}: Available concentrations of phosphorous and potassium;
CEC : Cation exchange capacity;
Ex.Ca, Ex.Mg and Ex.Na: Exchangeable of calcium, magnesium and sodium;
DTPA-Fe, DTPA-Mn,: DTPA-Cu and DTPA-Zn : Available nutrition trace elements of iron (Fe), manganese (Mn), copper (Cu), and zinc (Zn) were measured by diethylenetriaminepentaacetic acid (DTPA).
BD : Soil bulk density.

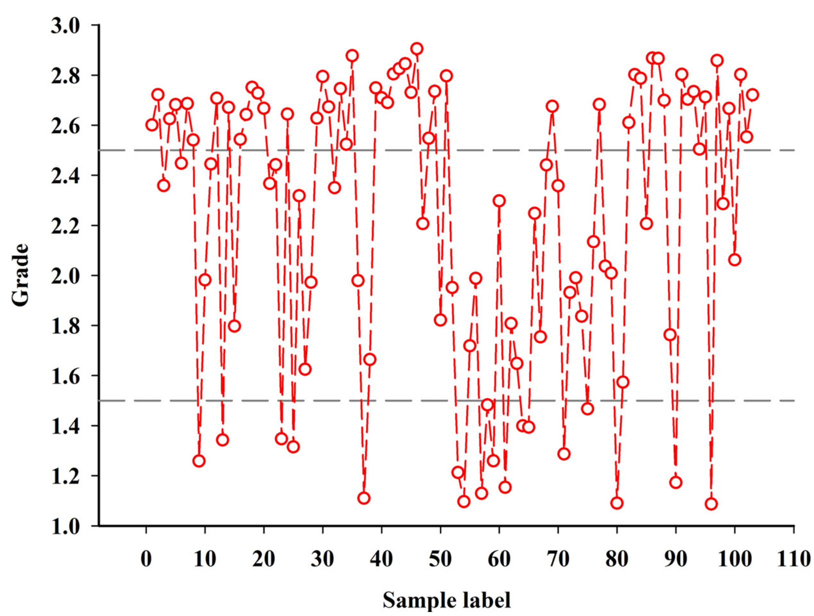

Fig. 3. Soil fertility quality classification based on the rice yield assessment standard.

K_T, and $P_{D,U} = 0$ indicates that the rice yield is distributed randomly; generally, the value of $P_{D,U}$ is between 0 and 1. A higher value indicates a greater influence of K_T on the rice yield.

The geodetector was used to identify the interaction between soil fertility indicators and the rice yield. Indicators X1 and X2 together might have an influence on Y (the rice yield) or affect Y independently. DP (X_1), DP (X_2), and DP ($X_1 \cap X_2$) are indicated in Table S1.

3. Results and discussion

3.1. Descriptive statistical analyses

The chemical and physical characteristics of the studied soils are summarized in Table 3. The mean value (± SD) of the surface soil pH was 4.80 (± 0.29), with the lowest coefficient of variation (CV) of 6.04%. The mean value (± SD) of the subsurface soil pH was 5.52 (± 0.54), with a CV of 9.86%, which indicates the universal acidification of soil in Jinxian County. The mean value of the surface SOM concentration in the study area was 33.63 ± 6.71 g kg^{-1}, which was

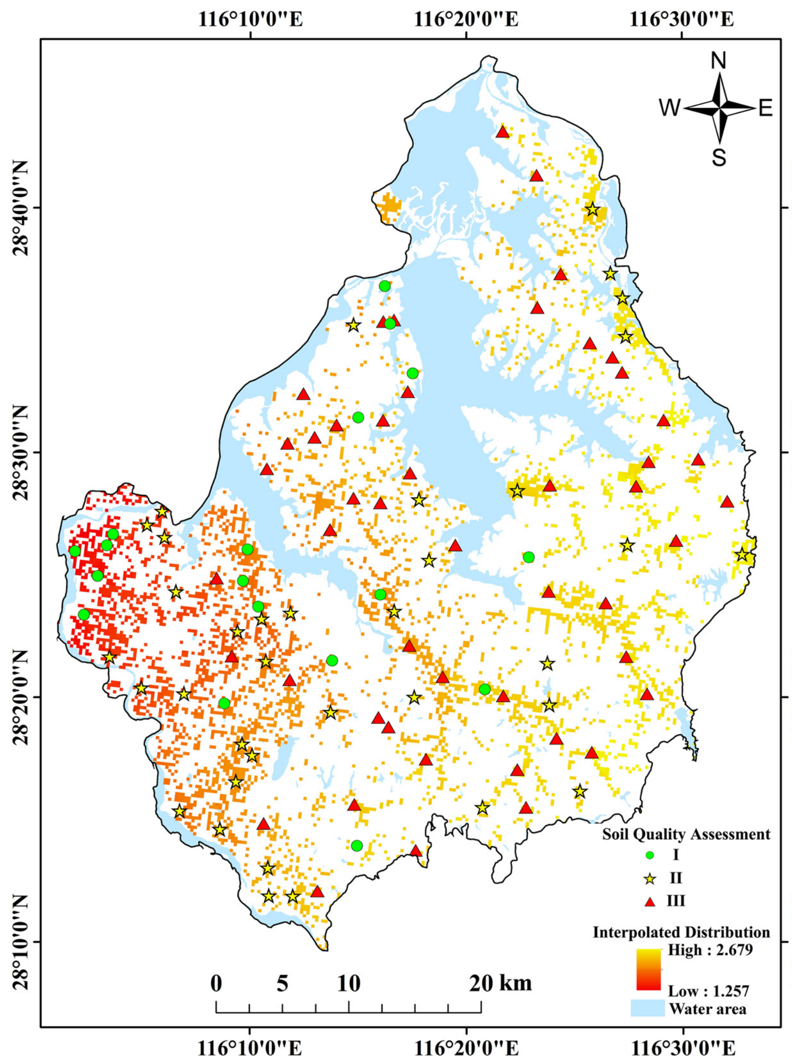

Fig. 4. Distribution of soil fertility quality in the study area.

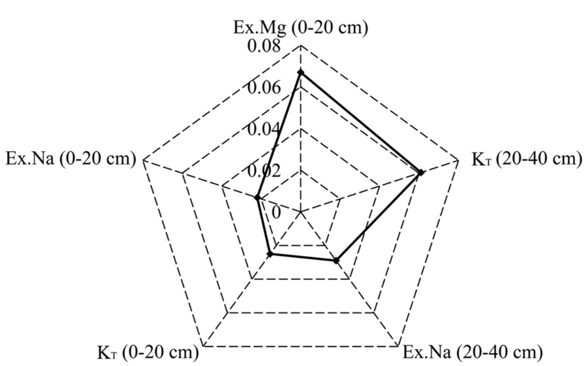

Fig. 5. Determination power values affecting the distribution of the rice yield.

relatively higher than that of the second national soil survey of Jinxian County in 1985 with a mean of 25.93 ± 7.78 g kg^{-1} (Soil of Jinxian County, 1985). Surface K_T was 13.95 ± 4.74, which indicated potassium deficiency in this area (Table S2). The concentration of soil exchangeable base cations was relatively low in the topsoil, with a mean CEC value of 10.23 ± 2.12 cmol kg^{-1}. The CV of Mn was the highest (98.23%) among all the topsoils, indicating the strongest spatial variation in this area. The BD of surface soil was slightly loose, while it was very compact in the subsurface soil. The soil in the study area was sticky, as the average silt/clay ratio of the surface soil was up to 2.51% and remained at 2.39% in the subsurface soil. The soil had serious soil acidification in the study area, and the SOM accumulated strongly in these soils.

3.2. Assessment of the soil fertility quality

Using the T-S fuzzy neural network model, an accurate and integrated soil fertility assessment was obtained (Fig. 3). We defined the soil samples with values under 1.5 as grade I, the soil samples with values between 1.5and 2.5 as grade II, and the soil samples with values higher than 2.5 as grade III. A total of 58% of the soil samples collected from Jinxian were categorized as grade III, which were located in the northeast and southeast of the study area. The results indicated that the soil fertility is poor in the eastern area, and is the poorest in southeastern area. Approximately 24% of the samples were in grade II, representing moderate soil fertility quality in Jinxian County. The remaining 18% of the soil samples that belonged to grade I with the best level of soil fertility quality, which were distributed in the southwest corner of the study area.

According to the test of the T-S fuzzy neural network model, the forecasted output was almost equal to the actual output and the error was between -0.05 and 0.05, indicating the excellent accuracy of the model (Figure S2). The spatial distribution of soil fertility quality was similar to that of the rice yield (Fig. 4). The lowest yield was observed in the southeastern area, and the highest was observed in the

Table 4
Interactive influence between pairs of indicators on rice yields.

Variable	Graphic form	Interaction	Correlation value
Ex.Mg (0-20 cm) ∩ K_T (20-40 cm)		Double indicator increase	0.0925
Ex.Mg (0-20 cm) ∩ Ex.Na (20-40 cm)		Double indicator increase	0.0780
Ex.Mg (0-20 cm) ∩ K_T (0-20 cm)		Double indicator increase	0.0737
Ex.Mg (0-20 cm) ∩ Ex.Na (0-20 cm)		Double indicator increase	0.0813
K_T (20-40 cm) ∩ Ex.Na (20-40 cm)		Nonlinear increase	0.1060
K_T (20-40 cm) ∩ K_T (0-20 cm)		Double indicator increase	0.0678
K_T (20-40 cm) ∩ Ex.Na (0-20 cm)		Nonlinear increase	0.0908
Ex.Na (20-40 cm) ∩ K_T (0-20 cm)		Nonlinear increase	0.0623
Ex.Na (20-40 cm) ∩ Ex.Na (0-20 cm)		Double indicator increase	0.0393
K_T (0-20 cm) ∩ Ex.Na (0-20 cm)		Nonlinear increase	0.0549

•$Min[DP(X_1)$ and $DP(X_2)]$ •$Max[DP(X_1)$ and $DP(X_2)]$ •$DP(X_1)+DP(X_2)$ ▾$DP(X_1 \cap X_2)$.

southwest. The results indicated that the soil fertility assessment based on the T-S fuzzy neural network model was not only statistically significant but also biologically relevant.

Furthermore, it was indicated that the selected soil fertility indicators were scientifically reliable based on GAM hypothesis test. The essential macro elements had no significant influence on the rice yield due to the excessive amounts of organic matter, nitrogen and phosphorus caused by long-term fertilization (Table S2). According to the CV values, pH and BD were rather uniformly distributed within the study area. Previous studies reported that an increase in BD would lead to soil compaction and a decrease in soil pH causes a major loss of soil potassium, calcium and magnesium (Letey, 1985; Xu et al., 2012; Najafi and Jalali, 2016). Hence, the decrease in the rice yield might partly be due to increasing and decreasing of soil BD and pH, respectively. Besides, pH and BD were not identified as explanatory variables which have no influence on the rice yield (*p*-value above 0.05). Although pH and BD were found to indirectly affect rice yields, they were not the main indicators affecting the distribution of rice yields in the study area. Therefore, these elements were not selected as fertility indicators.

3.3. Restricting indicators of soil fertility based on the geodetector model

The DP of the indicators can be ranked as follows (Fig. 5): Ex.Mg (0–20 cm) (0.067) > K_T (20–40 cm) (0.061) > Ex.Na (20–40 cm) (0.029) > K_T (0–20 cm) (0.025) > Ex.Na (0–20 cm) (0.022). This result indicates that the rice yield was mainly influenced by Mg in the surface soil and by K_T in the subsurface soil. Mg is the core element of chlorophyll, which is very important for plant photosynthesis (Farhat et al., 2016). Since the study area is rich in precipitation and potassium is easily loss, topsoil K_T deficiency was observed.

According to Table 4, the influence of two indicators on the spatial distribution of the rice yield was greater than the influence of a single indicator. The DP of Ex. Na (20–40 cm) ∩ K_T (20–40 cm) on the rice yield had the highest value ($P_{D,\ U}$ = 0.1060); the DPs of Ex.Mg (0–20 cm) ∩ K_T (20–40 cm) and Ex.Na (0–20 cm) ∩ K_T (20–40 cm) were 0.0925 and 0.0908, respectively. Na^+ is a beneficial element, for instance by replacing K^+ as a vacuolar osmoticum; furthermore, the K^+ and Na^+ ions could be transported across the plasmalemma and internal membranes with high or low ionic selectivity (Nievescordones et al., 2016). When potassium is scarce, this reabsorption is likely to result in increased root K^+ and Na^+ concentrations and thereby favor root growth in response to abiotic stresses (Gaymard et al., 1998). A nonlinear increase between sodium and potassium also indicated that different degrees of potassium deficiency were one of the most important reasons for the differences in the rice yield distribution. The uptake of nutrients in leaves, straw and grain was increased by K and Mg treatment (Brohi et al., 2000; Narendrababu et al., 2012; Ortas, 2017). The DP value of Ex.Mg (0–20 cm) ∩ K_T (20–40 cm) also suggested that proper use of potassium and magnesium fertilizers could increase rice yields in the study area.

4. Conclusion

An integrated soil fertility assessment and restricting indicator analysis of soil quality based on the rice yield were established in the study area.

Five indicators were selected using the GAM, including K_T (0–20 cm), Ex.Mg (0–20 cm), Ex.Na (0–20 cm), K_T (20–40 cm), and Ex.Na (20–40 cm). The selected soil fertility indicators were scientific and reliable for representing soil fertility from the productivity perspective. The assessment error of soil fertility was within ± 0.05. The result indicated that the spatial distribution of the soil fertility quality assessment based on the T-S fuzzy neural network model was similar to the spatial distribution of the rice yield.

Continuous fertilization for decades has improved the surface SOM concentrations in Jinxian County. However, this area still lacks potassium. Based on the results of the geodetector model, the rice yield could be increased by proper use of potassium and magnesium fertilizers in the study area.

These efficient and accurate models could help to fully understand the soil fertility quality in the study area and provide a theoretical basis for soil management and sustainable utilization. These models also can be used in other typical areas with appropriate calibrations.

Acknowledgment

The authors are grateful for the financial support from the National Key Technology R&D Program of China (grant number 2012BAD05B05).

Appendix A. Supplementary data

Supplementary material related to this article can be found, in the online version, at doi:https://doi.org/10.1016/j.still.2019.104322.

References

Amosa, M.K., Majozi, T., 2016. GAMS supported optimization and predictability study of a multi-objective adsorption process with conflicting regions of optimal operating conditions. Comput. Chem. Eng. 94, 354–361.
Blanes, V.V., Cantuaria, M.L., Nadimi, E.S., 2017. A novel approach for exposure assessment in air pollution epidemiological studies using neuro-fuzzy inference systems: comparison of exposure estimates and exposure-health associations. Environ. Res. 154, 196–203.
Brohi, A.R., Karaman, M.R., Topbaş, M.T., AKTAŞ, A., SAVAŞLI, E., 2000. Effect of potassium and magnesium fertilization on yield and nutrient content of rice crop grown on artificial siltation soil. Turk. J. Agric. For. 24, 429–436.
Farhat, N., Elkhouni, A., Zorrig, W., Smaoui, A., Abdelly, C., Rabhi, M., 2016. Effects of magnesium deficiency on photosynthesis and carbohydrate partitioning. Acta Physiol. Plant. 38, 145.
Fan, Y.N., Yao, L.P., Qu, M.K., Hu, W.Y., Huang, B., Zhao, Y.C., 2017. Yield-based soil fertility quality assessment and constraint factor-based zoning of paddy soil—a case study of Jinxian County. Acta Pedologica Sinica 54, 1157–1169 (in Chinese).
Gaymard, F., Pilot, G., Lacombe, B., Bouchez, D., Bruneau, D., Boucherez, J., Michaux-Ferrie`re, N., Jean-Baptiste Thibaud, J.B., Sentenac, H., 1998. Identification and disruption of a plant shaker-like outward channel involved in K^+ release into the

xylem sap. Cell 94, 647–655.
Hastie, T., Tibshirani, R., 1986. Generalized additive models. Technometrics 1, 297–310.
Hou, T., 2011. The application of fuzzy neural network based on T-S model in SanChuan Water quality evaluation. Energy Energy Conserv. 6, 54–56 (in Chinese).
Hu, D., Shu, X., Yao, B., Cao, Q., 2014. The evolvement of spatio-temporal pattern of per capita grain Possession in counties of Jiangxi Province. Areal Res. Dev. 33, 157–162 (in Chinese).
Huang, B., Shi, X., Yu, D., Öborn, I., Blombäck, K., Pagella, T.F., Wang, H., Sun, W., Sinclair, F.L., 2006. Environmental assessment of small-scale vegetable farming systems in peri-urban areas of the Yangtze River Delta Region, China. Agr. Ecosyst. Environ. 112, 391–402.
Jiang, X.Y., Zhang, Q., Xie, Z.D., 2010. Distribution and abundance or deficiency assessment of the surface soil nutrient elements in Poyang Lake and its surrounding economic area. Geol. Surv. Res. 33, 226–231 (in Chinese).
Juhos, K., Szabó, S., Ladányi, M., 2016. Explore the influence of soil quality on crop yield using statistically-derived pedological indicators. Ecol. Indic. 63, 366–373.
Kaniu, M.I., Angeyo, K.H., 2015. Challenges in rapid soil quality assessment and opportunities presented by multivariate chemometric energy dispersive X-ray fluorescence and scattering spectroscopy. Geoderma 241-242, 32–40.
Lai, Q.W., Liu, X., Huang, Q.H., 1989. The genesis of paddy soil gleization and its amendment strategy in Poyong-Lake Region, China. Scientia Agricultura Sinica 22, 65–74 (in Chinese).
Letey, J., 1985. Relationship between soil physical properties and crop production. Advances in Soil Science. Springer, New York.
Liu, J., Wu, L.C., Chen, D., Li, M., Wei, C.J., 2017. Soil quality assessment of different *Camellia oleifera* stands in mid-subtropical China. Appl. Soil Eco. 113, 29–35.
Liu, Y., Wang, H., Zhang, H., Liber, K., 2016. A comprehensive support vector machine-based classification model for soil quality assessment. Soil Till. Res. 155, 19–26.
Lu, R.K., 2000. Analytical Methods of Agricultural Chemistry in Soil. China Agricultural Scientech Press, Beijing, China (in Chinese).
Merrill, S.D., Liebig, M.A., Tanaka, D.L., Krupinsky, J.M., Hanson, J.D., 2013. Comparison of soil quality and productivity at two sites differing in profile structure and topsoil properties. Agr. Ecosyst. Environ. 179, 53–61.
Najafi, S., Jalali, M., 2016. Effect of heavy metals on pH buffering capacity and solubility of Ca, Mg, K, and P in non-spiked and heavy metal-spiked soils. Environ. Monit. Assess. 188, 1–11.
Narendrababu, B., Kumar, S.A., Sudhir, K., 2012. Effect of graded doses of potassium with sulphur and/or magnesium on yield of potato and cabbage and soil nutrient status. Mysore Journal of Agricultural Sciences 46, 274–280.
Nelson, D.W., Sommers, L.E., Sparks, D.L., Page, A.L., Helmke, P.A., Loeppert, R.H., Soltanpour, P.N., Tabatabai, M.A., Johnston, C.T., Sumner, M.E., 1996. Total carbon, organic carbon, and organic matter. Methods Soil Analysis 9, 961–1010.
Nelson, E., Mendoza, G., Regetz, J., Polasky, S., Tallis, H., Cameron, D.R., et al., 2009. Modeling multiple ecosystem services, biodiversity conservation, commodity production, and tradeoffs at landscape scales. Front. Ecol. Environ. 7, 4–11.
Nievescordones, M., Al Shiblawi, F.R., Sentenac, H., 2016. Roles and transport of sodium and potassium in plants. Met. Ions Life Sci. 16, 291–324.
Ortas, I., 2017. Influence of potassium and magnesium fertilizer application on the yield and nutrient accumulation of maize genotypes under field conditions. J. Plant Nutr. 41, 1–10.
Qi, Y., Darilek, J.L., Huang, B., Zhao, Y., Sun, W., Gu, Z., 2009. Evaluating soil quality indices in an agricultural region of Jiangsu Province, China. Geoderma 149, 325–334.
Rahmanipour, F., Marzaioli, R., Bahrami, H.A., Fereidouni, Z., Bandarabadi, S.R., 2014. Assessment of soil quality indices in agricultural lands of Qazvin province, Iran. Ecol. Indic. 40, 19–26.
Raiesi, F., 2017. A minimum data set and soil quality index to quantify the effect of land use conversion on soil quality and degradation in native rangelands of upland arid and semiarid regions. Ecol. Indic. 75, 307–320.
Rodríguez, E., Peche, R., Garbisu, C., Gorostiza, I., Epelde, L., Artetxe, U., Irizar, A., Soto, M., Becerril, J.M., Etxebarria, J., 2016. Dynamic quality index for agricultural soils based on fuzzy logic. Ecol. Indic. 60, 678–692.
Rojas, J.M., Prause, J., Sanzano, G.A., Arce, O.E.A., Sánchez, M.C., 2016. Soil quality indicators selection by mixed models and multivariate techniques in deforested areas for agricultural use in NW of Chaco, Argentina. Soil Till. Res. 155, 250–262.
Song, L.K., Wen, J., Fei, C.W., Bai, G.C., 2018. Distributed collaborative probabilistic design of multi-failure structure with fluid-structure interaction using fuzzy neural network of regression. Mech. Syst. Signal Pr. 104, 72–86.
Toebe, M., Filho, A.C., 2013. Multicollinearity in path analysis of maize (*Zea mays L.*). J. Cereal Sci. 57, 453–462.
Vasu, D., Singh, S.K., Ray, S.K., Duraisami, V.P., Tiwary, P., Chandran, P., Nimkar, A.M., Anantwar, S.G., 2016. Soil quality index (SQI) as a tool to evaluate crop productivity in semi-arid Deccan plateau, India. Geoderma 282, 70–79.
Viana, R.M., Ferraz Jr, J.B.S., A.F.N, Vieira, G., Pereira, B.F.F., 2014. Soil quality indicators for different restoration stages on amazon rainforest. Soil Till. Res. 140, 1–7.
Wang, J.F., Xu, C.D., 2017. Geodetector: principle and prospective. Acta Geographica Sinica 72, 116–134 (in Chinese).
Wang, J.F., Li, X.H., Christakos, G., Liao, Y.L., Zhang, T., Gu, X., Zheng, X.Y., 2010. Geographical detectors-based health risk assessment and its application in the neural tube defects study of the heshun region. China. Int. J. Geogr. Inf. Sci. 24, 107–127.
Wood, S., 2006. Generalized additive models: an introduction with R. J. Stat. Softw. 6, 1–3.
Wolde, Z., Haile, W., 2015. Phosphorus sorption isotherms and external phosphorus requirements of some soils of southern Ethiopia. Afr. Crop Sci. J. 23, 89–99.
WRB, 2015. World Reference Base for Soil Resources 2014, Update 2015. International Soil Classification System for Naming Soils and Creating Legends for Soil Maps. World Soil Resources Reports No. 106. FAO, Rome.
Wu, J., Yang, P., Zhang, X., Shen, Z., Yu, C., 2015. Spatial and climatic patterns of the relative abundance of poisonous vs. non-poisonous plants across the Northern Tibetan Plateau. Environ. Monit. Assess. 187, 491.
Xu, R.K., Zhao, A.Z., Yuan, J.H., Jiang, J., 2012. pH buffering capacity of acid soils from tropical and subtropical regions of China as influenced by incorporation of crop straw biochars. J. Soil Sediment 12, 494–502.
Xu, Z., Wang, F., Han, Y., Zhang, G., Wang, J., 2013. Regional agriculture drought risk assessment based on T-S fuzzy neural network. Int. J. Appl. Environ. Sci. 8, 2295–2307.
Yan, X., Luo, X., 2016. Assessment of the soil quality by fuzzy mathematics in farmland around a uranium mill tailing repository in China. Radioprotection 51, 37–41.
Yao, L.P., Huang, B., Sun, W.X., 2015. Limiting soil factors on rice yield in typical Area of Poyang Lake Region, China. Soil 47, 675–681 (in Chinese).
Yi, Y., Sun, J., Zhang, S., Yang, Z., 2016. Assessment of Chinese sturgeon habitat suitability in the Yangtze River (China): comparison of generalized additive model, data-driven fuzzy logic model, and preference curve model. J. Hydrol. 536, 447–456.
Zhang, Y., 2012. Application of T-S fuzzy neural network based on declination compensation in soft sensing. Math. Comput. Simulat. 86, 92–99.
Zhang, G., Bai, J., Xi, M., Zhao, Q., Lu, Q., Jia, J., 2016. Soil quality assessment of coastal wetlands in the Yellow River Delta of China based on the minimum data set. Ecol. Indic. 66, 458–466.
Soil of Jinxian County, 1985. Agricultural Zoning Committee of Jinxian County, Jiangxi Province (in Chinese). .